Title

Metal artifact suppression at the hip: diagnostic performance at 3.0 T versus 1.5 Tesla



Journal

Skeletal Radiology, 44(11)

ISSN

0364-2348

Authors

Nardo, Lorenzo

Han, Misung

Kretschmar, Martin

et al.

Publication Date

2015-11-01

DOI

10.1007/s00256-015-2214-5

Peer reviewed

Skeletal Radiol (2015) 44:1609–1616
DOI 10.1007/s00256-015-2214-5

SCIENTIFIC ARTICLE

# Metal artifact suppression at the hip: diagnostic performance at 3.0 T versus 1.5 Tesla

**Lorenzo Nardo[1] · Misung Han[1] · Martin Kretschmar[1] · Michele Guindani[2] · Kevin Koch[3,4] · Thomas Vail[5] · Roland Krug[1] · Thomas M. Link[1]**

Received: 26 February 2015 / Revised: 19 May 2015 / Accepted: 30 June 2015 / Published online: 23 July 2015


**Abstract**
*Purpose* This work aimed to compare the diagnostic performance of a metal artifact suppression sequence (MAVRIC-SL) for imaging of hip arthroplasties (HA) at 1.5 and 3 Tesla (T) field strength.
*Methods* Eighteen patients (10 females; aged 27–74) with HA were examined at 3.0 and 1.5 T within 3 weeks. The sequence protocol included 3D-MAVRIC-SL PD (coronal), 3D-MAVRIC-SL STIR (axial), FSE T1, FSE PD and STIR sequences. Anatomical structures and pathological findings were assessed independently by two radiologists. Artifact extent and technical quality (image quality, fat saturation and geometric distortion) were also evaluated. Findings at 1.5 and 3.0 T were compared using a Wilcoxon signed rank test.
*Results* While image quality was better at 1.5 T, visualization of anatomic structures and clinical abnormalities was not significantly different using the two field strengths ($p>0.05$). Fat suppression and amount of artifacts were significantly better at 1.5 T ($p<0.01$). Inter- and intra-reader agreement for different anatomic details, image quality and visualization of abnormalities ranged from $k=0.62$ to $k=1.00$.
*Conclusion* MAVRIC-SL at 1.5 T had a comparable diagnostic performance when compared MAVRIC-SL at 3.0 T; however, the higher field strength was associated with larger artifacts, limited image quality and worse fat saturation.

**Keywords** Hip · Pain · Surgery · MRI

## Introduction

A recent meta-analysis of the literature demonstrated that hip arthroplasty (HA) improved mid-term health-related quality of life and resulted in good patient satisfaction and substantial functional gains [1]. In 2005, over 200,000 hip arthroplasty

✉ Lorenzo Nardo
Lorenzo.Nardo@ucsf.edu

Misung Han
Han.Misung@ucsf.edu

Martin Kretschmar
Martin.Kretschmar@ucsf.edu

Michele Guindani
mguindani@mdanderson.org

Kevin Koch
kmkoch@mcw.edu

Thomas Vail
vailt@orthosurg.ucsf.edu

Roland Krug
Roland.Krug@ucsf.edu

Thomas M. Link
thomas.link@ucsf.edu

[1] Musculoskeletal and Quantitative Imaging Research, Department of Radiology and Biomedical Imaging, University of California San Francisco, 185 Berry street, suite 350, San Francisco, CA 94107, USA

[2] Department of Biostatistics – Unit 1411, The University of Texas MD Anderson Cancer Center, P.O. Box 301402, Houston, TX 77230-1402, USA

[3] Department of Biophysics, Medical College of Wisconsin, 8701 Watertown Plank Rd, Milwaukee, WI 53226, USA

[4] Department of Radiology, Medical College of Wisconsin, 8701 Watertown Plank Rd, Milwaukee, WI 53226, USA

[5] Department of Orthopedic Surgery, University of California San Francisco, 500 Parnassus Avenue, MU320, San Francisco, CA 94143, USA

procedures were performed and this number is expected to double by 2026 [2, 3]. However, after hip replacement, a large number of patients experience pain due to complications from the surgery [4–6]. The detection rate of hip arthroplasty complications has increased using advanced imaging techniques, which critically impacts patient management [7]. The rate of hip arthroplasty revisions has increased 60 % from 2005 and is projected to increase to 137 % by 2030 [2, 3].

While radiography is always the first step in assessing potential complications, MRI offers substantial benefits in better characterizing complications such as aseptic lymphocytic vasculitis-associated lesions (ALVAL), adverse reaction to metal debris [8], osteolysis, peri-prosthetic stress fractures, synovitis, impingement and infections. Recently developed metal artifact suppression MRI sequences have enabled MRI to become a crucial tool in the follow-up of patients with hip prosthesis [9]. Different metal suppression sequences have been developed including slice-encoding metal artifact correction (SEMAC) [10], multi-acquisition with variable resonance imaging combination (MAVRIC) [11], and a hybrid technique of those approaches termed MAVRIC-SL [12].

These three-dimensional multispectral imaging sequences (3D-MSI) were originally developed for 1.5 T and have demonstrated significant reduction of susceptibility artifacts near metal implants. However, with the increasing use of 3.0 T magnetic field strength for musculoskeletal imaging applications, several studies have also aimed at showing feasibility of these techniques at 3.0 T [13, 14]. Two previous studies have demonstrated that effective metal artifact reduction was possible at both 1.5 and 3.0 T, but it was performed in vitro using animal specimens [14, 15]; however, to the best of our knowledge to date no study was published directly comparing MAVRIC imaging at 1.5 and 3.0 T in vivo in the same patients with hip prosthesis.

The aim of our study was therefore to directly compare imaging of patients with HA at 1.5 and 3.0 T MRI using MAVRIC sequences specifically investigating the visualization of anatomical structures, the detection of clinical abnormalities, artifact reduction and image quality. Based on previous studies our hypothesis was that the diagnostic performance of MAVRIC-SL sequences is similar at 1.5 and 3 T.

## Materials and methods

### Patient population

This HIPAA compliant study was approved by the committee on human research (CHR) at our institution and informed consent was acquired from each subject before the MRI scans. Inclusion criteria aimed to select a population of patients who had undergone HA and presented at the Arthroplasty Clinic of our Department of Orthopedic Surgery with symptoms of hip pain not explained by standard radiographs and concerning for synovitis, osteolysis with loosening and ALVAL disease. Furthermore exclusion criteria applied to the enrollment were: (1) age<18 years, (2) claustrophobia, (3) pregnancy and (4) pacemaker or any implanted devices (ex. insulin pump), which contraindicated MRI scan. In the patients included in this study, MRI scans at both 1.5 and 3 T were obtained within 3 weeks. Initially a total number of 35 patients were enrolled, but only 18 patients completed both 1.5 and 3 T MRI scans within 3 weeks and, thus, were eventually included in our final analysis. Sixteen patients did not complete the second MRI scan, and one patient did not complete the first scan due to claustrophobia.

Our cohort consisted of 8 men and 10 women. The mean age at the time of the study was 58.9 years, spanning between 27 to 74 years with a standard deviation of 12.5. Patients with two types of implants were included: hip resurfacing ($n$=4) and total hip replacements ($n$=14). The hip resurfacing consisted of chromium-cobalt prostheses. The total hip replacement prostheses were metal-on-plastic ($n$=3), ceramic-on-metal ($n$ =4) and metal-on-metal ($n$=7); the prostheses were implanted at different time points for each patient, spanning from 12 months to 8 years. All patients reported symptoms of constant dull or sharp hip pain (2 mild, 10 moderate and 6 severe) along with stiffness ($n$=12), feeling of instability ($n$=3), clicking of the hip ($n$=2) and sleeping problems related to hip pain ($n$=1) for at the last 6 months.

In eight patients (44.4 %), radiographs of the hip/pelvis were obtained at our institution within 6 months prior to the MRI scans. Seven patients had unremarkable radiographs, showing the correct alignment of the implant without signs of loosening or infection. Only one patient had an abnormal hip radiographs demonstrating soft tissue calcifications around the prosthesis. In all other 10 patients radiographs were performed at outside institutions and in none of these patients were clinical findings explained by these radiographs.

### Image acquisition

In each patient, the 1.5 T scan was performed on a Signa Excite scanner (GE Healthcare, Waukesha, WI) using an eight-channel phased-array cardiac coil (USA Instruments, Aurora, OH), and the 3.0 T scan was performed on a Discovery MR750 scanner (GE Healthcare, Waukesha, WI) using an eight-channel phased-array cardiac coil (In-Vivo Corporation, Gainesville, FL). The MRI protocol included a proton density (PD)-weighted coronal 2D fast spin echo (FSE) sequence, axial 2D FSE sequence with short T1 inversion recovery (STIR) fat suppression, PD-weighted coronal MAVRIC-SL sequence, and axial MAVRIC-SL sequence with STIR fat suppression. For the STIR fat suppression, the inversion time was 150 ms at 1.5 T and 170 ms at 3 T considering increased T1 at 3.0 T. In order to correct for the longer T1 recovery time

**Table 1** MRI protocol at 1.5 T (*top*) and 3.0 T (*bottom*)

| 1.5 Tesla | TR (ms) | TE (ms) | Sl Thk (mm) | FOV readout (cm) | Echo train length | Averages | Bandwidth (kHz) | No. of slices | Matrix | Scan time (min) |
|---|---|---|---|---|---|---|---|---|---|---|
| Axial T1 FSE | 700 | 6.2 | 4 | 40–48 | 4 | 4 | ±125 | 37 | 320–224 | 5 |
| Coronal STIR FSE | 3,150 | 44 | 4 | 44 | 16 | 4 | ±100 | 25 | 288 × 224 | 9 |
| Axial STIR FSE | 4,000 | 40 | 4 | 40–48 | 16 | 4 | ±100 | 23 | 288 × 179 | 9–12 |
| Coronal PD MAVRIC-SL | 2,000 | 28 | 3.2 | 40–48 | 16 | 1 | ±125 | 40 | 384 × 256 | 5 |
| Axial STIR MAVRIC-SL | 3,500 | 33 | 3.6 | 40–48 | 16 | 1 | ±125 | 52 | 320 × 179 | 11 |
| 3 Tesla | | | | | | | | | | |
| Axial T1 FSE | 600 | 6.2 | 4 | 36–38 | 4 | 8 | ±125 | 37 | 416 × 224 | 6 |
| Coronal STIR FSE | 5,000–7,000 | 50 | 4 | 36–38 | 18 | 6 | ±125 | 31 | 384 × 192 | 6 |
| Axial STIR FSE | 5,000 | 36 | 4 | 40–48 | 16 | 4 | ±100 | 35 | 288 × 179 | 9 |
| Coronal PD MAVRIC-SL | 2,000 | 27 | 3.2 | 40–48 | 16 | 1 | ±125 | 40 | 384 × 320 | 10 |
| Axial STIR MAVRIC-SL | 5,000–7,000 | 42 | 3.2 | 40–48 | 24 | 1 | ±125 | 44 | 320 × 134 | 11 |

at the higher field strength, the inversion time was slightly increased. The standard 2D FSE sequences were also optimized for imaging around metal, which included the use of a maximum readout receiver bandwidth. Furthermore, STIR fat suppression was used for both 2D FSE and MAVRIC-SL instead of frequency selective fat suppression techniques, due to large field inhomogeneities near metals. The imaging protocols and pertinent imaging parameters for both 1.5 and 3.0 T are presented in Table 1.

## Image analysis

Anatomical structures, clinical abnormalities and technical quality were graded by two board certified radiologists (L.N. and M.K.), separately. To better standardize image analysis, initially the calibration sessions were performed by three radiologists (L.N., M.K. and T.M.L.) using 10 MRI studies obtained in patients with total hip prosthesis that were not included in the final study population. Sequences were analyzed randomly and radiologists were blinded to the image parameters in particular to the field strength.

A 5-point grading system was used to evaluate the following anatomical structures [13]: greater trochanter, lesser trochanter, femoral head and neck, acetabulum, sciatic nerve and iliopsoas muscles. A grade of (5) was defined as good delineation of anatomic structures; grade (4) as anatomic structure fully visible with slight blurring of borders; grade (3) as anatomic structure fully visible but significant blurring of borders; grade (2) as anatomic structure only partially visible, and grade (1) as anatomic structure not visible. An example for the grading is provided in Fig. 1.

*Image quality* was visually assessed in regard to signal-to-noise ratio, blurring, spatial resolution and contrast; again a 5-grade quality score was used [13, 15]. Figure 2 provides an example of good image quality. *Fat saturation and geometric distortion* were scored separately. Very good image quality (5) was defined as clear visibility of anatomic details with sharp contours, no areas of blurring and obvious differences in

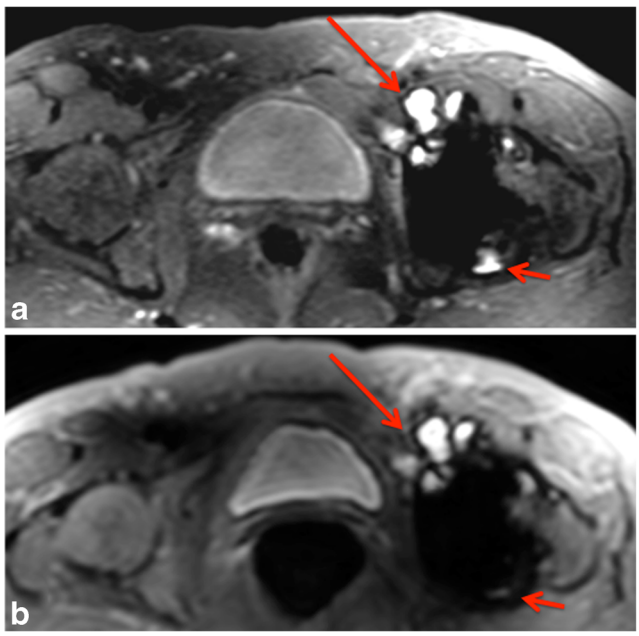


**Fig. 1** Axial MAVRIC-SL STIR images at 1.5 T (**a**), 3.0 T (**b**). Iliopsoas bursitis (*long arrows*) is noted at both magnetic field strengths. The small amount of fluid in the posterior aspect of the joint (*short arrows*) is better appreciated at 1.5 T where the metal artifact was smaller. The greater trochanter is partially affected by artifacts on both images and it was scored 2 at 1.5 T and 3 at 3.0 T

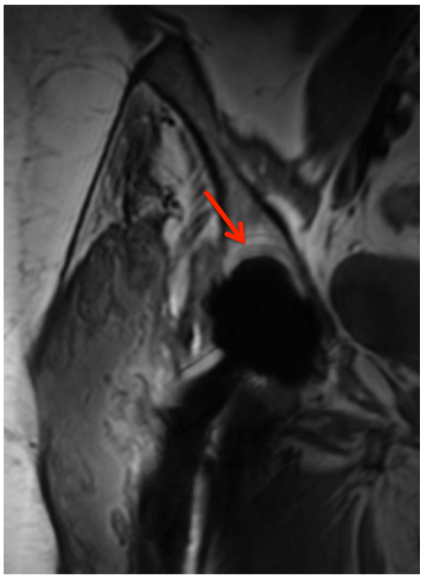

**Fig. 2** Coronal proton density weighted MAVRIC SL image at 3.0 T demonstrates minimal geometrical distortion (*arrow*), good signal-to-noise ratio, no blurring and size of the artifact mirroring the shape of the implant

signal intensity. Good image quality (4) was defined as mild loss of contrast without impairment of visibility of image details. Fair image quality (3) was defined as moderate contrast and mild blurring that mildly affected the discrimination of anatomic details. Poor image quality (2) was defined as moderate contrast and blurring with only vague discrimination of anatomic details like vessels of nerves, image quality was defined as very poor (1) when anatomic details were obscured by low contrast and blurry contours. Quality of fat saturation was graded as the following: 5=complete fat suppression with homogenously low signal in the bone marrow or subcutaneous fat, 4=mild inhomogeneity of low fat signal that did not affect the evaluation of the image, 3=moderate inhomogeneity mildly impairing the image evaluation, 2=intermediate and inhomogeneous signal intensity of fatty tissue definitely impairing image evaluation, 1=missing fat saturation with subcutaneous fat and bone marrow appearing markedly brighter compared to muscle tissue. An example is provided in Fig. 3. Geometric distortion was graded as 5=not present, 4=minimal distortion that did not impair anatomic evaluation (Fig. 2), 3=distortion mildly altering anatomic contours, 2=distortion severely impairing anatomic evaluation near the metal implant and 1=distortion making anatomic evaluation of structures surrounding the implant impossible. In addition, the *extent of the artifact* was defined as the area of severe signal loss that obscured any anatomic information [13]. It was measured on the slice with the maximum extent of artifact in two dimensions (square centimeter, $cm^2$) as demonstrated in Fig. 4.

*Clinical abnormalities* recorded included joint effusion, aseptic lymphocyte-dominated vasculitis-associated lesions (ALVAL), synovitis and bursitis, bone marrow edema pattern, osteolysis and insertion tendinopathy at the greater trochanter. Joint effusion was defined as abnormal presence of fluid (greater than 7 mm in thickness) within the joint as described by Lee et al. [15]. ALVAL was defined as a soft tissue mass or fluid-filled cavity with thickened low intensity capsule in the periarticular region with joint effusion bursitis and possible remodeling of the adjacent bone as previously described [16]. An example is provided in Fig. 5. Bursitis was defined as an accumulation of fluid in the iliopsoas, trochanteric or ischiotrochanteric bursae, which is normally not evident on MRI images (Fig. 6). Bone marrow edema pattern was defined as increased signal in the bone marrow in fluid sensitive images and low signal on T1W images. Osteolysis was defined as endosteal, intracortical, or non-linear cancellous bone destruction detected as high signal intensity in fluid sensitive sequence (Fig. 4) [13]. Insertion tendinopathy demonstrated signal alteration within the insertion of the gluteal muscles at the greater tuberosity with thickening of the muscle tendons.

The images obtained in the corresponding plane at 1.5 and 3.0 T were graded by two radiologists (L.N. and M.K.) independently; a consensus reading with a third radiologist

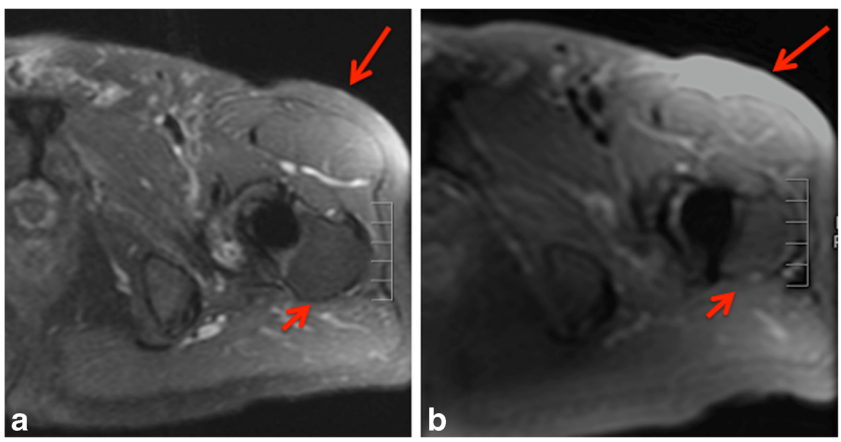


**Fig. 3** Axial MAVRIC-SL STIR images at 1.5 T (**a**) and 3.0 T (**b**). Anatomy of the femoral greater trochanter was scored as 3 at 3.0 T and as 5 at 1.5 T (*short arrow*). Fat saturation (*long arrows*) is limited at 3.0 T (scored as 1), while on the 1.5 T image fat suppression is of substantially higher quality (scored as 3)

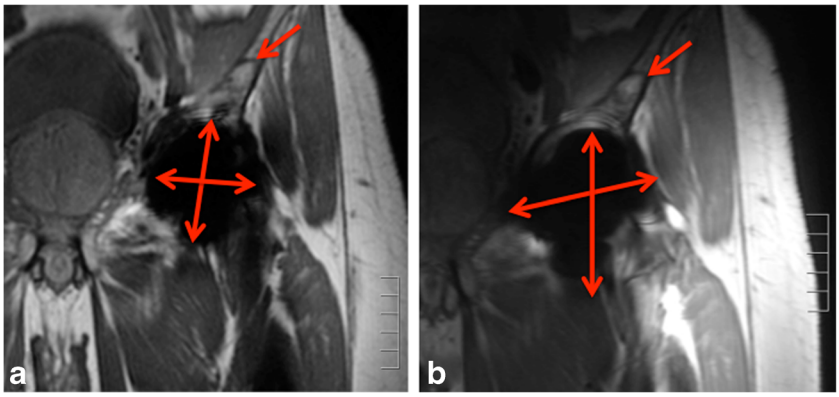


**Fig. 4** Coronal proton density-weighted MAVRIC images at 1.5 T (**a**) and 3.0 T (**b**). Small area of osteolysis was demonstrated at both field strengths (*arrows*). The size of signal voids at 1.5 T (5.1×4.8 cm) is markedly smaller compared to the artifact size at 3.0 T (8.2×7.8 cm); however, this did not affect the ability to show the lesion at 3.0 T. The acetabular area is markedly impacted by metal artifacts on both images; it was given a score of 1 on the coronal images

(T.M.L.) was performed in case of disagreement. As a measure of the *reproducibility* of the grading systems used in this study, all patients studies were scored again 3 weeks after the initial readings by one of the radiologists (L.N.) and intra-reader reproducibilities were calculated.

### Statistical analysis

After comparing grading obtained, independently, in the coronal and in the axial plane, the highest score was chosen for every investigated parameter. Wilcoxon signed rank tests were performed to detect differences in the grades of different MRI variables assessed for the MAVRIC-SL images obtained at 1.5 and 3.0 T. A significance level of $\alpha$=0.05 was considered to reject the null hypothesis of no difference between MAVRIC-SL images obtained at 1.5 and at 3.0 T ($p$<0.05). Inter- and Intra-rater agreement of categorical variables was determined by calculation of Cohen's kappa values, whereas the intra-class correlation coefficient was computed for the quantitative artifact measurements.

## Results

### Anatomical structures

Though scores at 1.5 T were consistently higher than at 3.0 T, there were no statistically significant differences in the visualization of anatomical structures when MAVRIC-SL sequences obtained at 1.5 T were compared to MAVRIC-SL at 3.0 T: specifically, $p$ values were greater than 0.05 for all considered variables (Table 2). Higher scores at 1.5 T were found for the assessment of the lesser tuberosity areas—4.6 (1.5 T) and 4.4 (3.0 T) with $p$>0.05—and the greater tuberosity—4.6 (1.5 T) and 4.7 (3.0 T) with $p$>0.05—as shown in Fig. 4. The acetabular area demonstrated the lowest scores with 3.5 at 1.5 T and 3.3 at 3.0 T ($p$>0.05) as demonstrated on Fig. 4.

### Comparison of technical quality and artifact extent

When MAVRIC SL sequences acquired at 3.0 and 1.5 T were compared, significantly larger artifact size and worse fat saturation scores were found at 3 T, while scores for geometric distortion and image quality were not significantly different (Table 3). The average artifact size measured 58.8 cm$^2$ at 3 T while it measured 42.2 cm$^2$ at 1.5 T ($p$<0.001). Fat

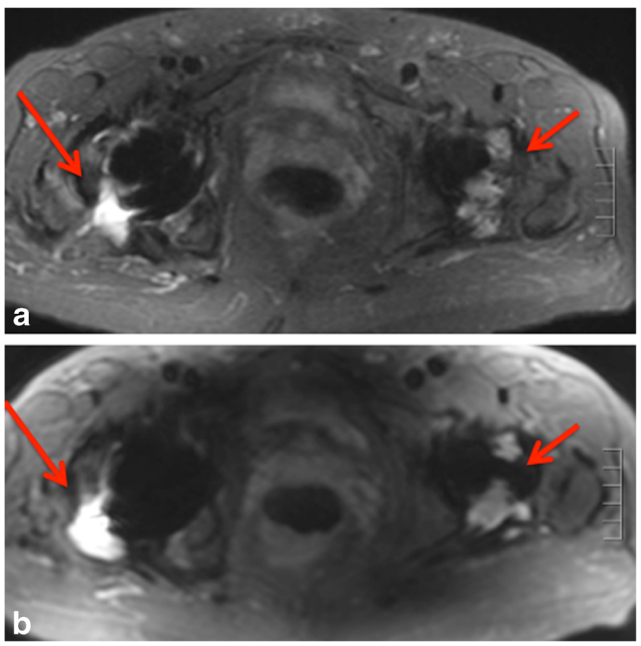


**Fig. 5** Axial MAVRIC-SL STIR images at 1.5 T (**a**) and 3.0 T (**b**). ALVAL abnormality on the left (*short arrows*) and right hip joint effusion (*long arrows*) are noted at both magnetic field strengths. The fat saturation was better at 1.5 T (scored as 3) than at 3.0 T (scored as 1). The greater tuberosity is well seen at both field strengths with a score of 5

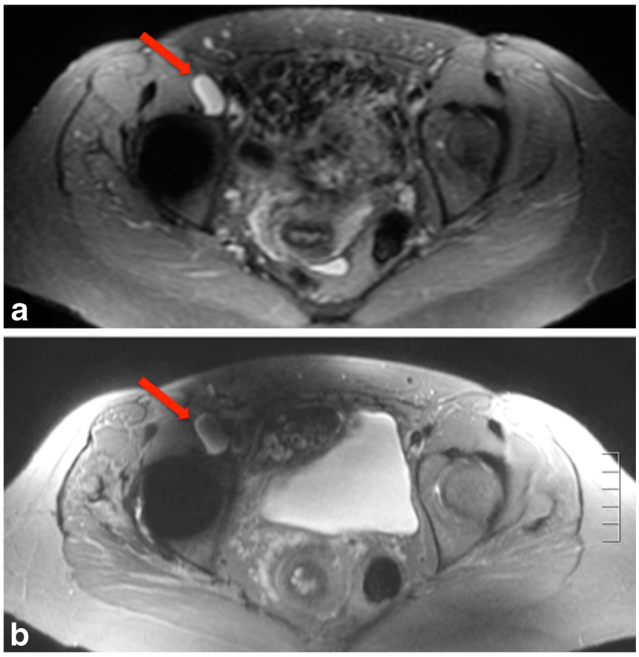


**Fig. 6** Axial MAVRIC-SL STIR images at 1.5 T (**a**) and 3.0 T (**b**) demonstrate iliopsoas bursitis (*arrows*). 3.0 T image shows less efficient fat-saturation when compared to 1.5 T image. Fat saturation scores were 3 and 1, at 1.5 and 3.0 T, respectively. Shading artifact is noted in the area anterior and medial to the hip replacement at 3.0 T; however, this artifact does not entirely compromise the detection of the abnormality and is likely due to the shading artifact related to the B1 magnetic field. Iliopsoas muscle was affected by a strong artifact at 3.0 T and scored as 2, while it was scored as a 3 on the 1.5 T image

suppression scores were 2.9 at 3 T and 3.7 at 1.5 T ($p$=0.001). Image quality and geometrical distortions had worse average scores using MAVRIC obtained at 1.5 T than 3.0 T MAVRIC; however, the $p$ values for these comparisons did not reach statistical significance. Details are reported in Table 3.

### Pathological abnormalities

All pathological abnormalities were recorded and presented in Table 4. There were no differences in the number or type of abnormalities seen on MAVRIC SL sequences at 1.5 and at 3.0 T; specifically, all of the abnormalities detected at one field strength were also seen at the other field strength even if artifacts affected the abnormalities. For example on Fig. 6, an example of iliopsoas bursitis is presented at both 3.0 and 1.5 T. The abnormality is seen at both field strengths although at 3.0 T it is moderately affected by artifacts.The most frequent abnormalities noted were joint effusion and iliopsoas bursitis (Fig. 1), which were noted in 9 and 11 patients, respectively. Also cases of ALVAL tumors ($n$=2; Fig. 5) and osteolysis ($n$=3; Fig. 4) were detected both at 1.5 and 3 T.

### Reproducibility of measurements

As shown in details in Table 5, inter- and intra-rater agreement kappa values for gradings of anatomical structures, image quality variables and pathological abnormalities ranged from 0.62 to 1.0 (mean=0.88, 95 % CI: 0.62–1.0). The intra class correlation coefficient for the artifact size ranged from 0.87 to 1.0 (mean=0.96, 95 % CI=0.88–1.0).

## Discussion

In this study, we investigated the reduction of metal artifacts in MR images of patients with HA using a novel MAVRIC-SL sequence at 1.5 and 3 T. Our data demonstrated that the diagnostic performance in evaluating abnormalities around hip prosthesis was similar at 1.5 and 3.0 T; we also found similar performance in the visualization of anatomical features. However, MAVRIC at 1.5 T demonstrated more efficient fat suppression and artifact size was significantly reduced improving overall image quality.

To the best of our knowledge, this is the first clinical study directly comparing metal reduction sequences in patients with hip prosthesis at 1.5 and 3.0 T field strength. Most publications do not recommend 3.0 T for imaging of tissues around prosthesis because induced local static magnetic field offsets are expected to double when switching from 1.5 to 3.0 T and result in larger susceptibility artifacts. However, some publications have recently indicated the feasibility of metal suppression sequences at 3.0 T [14, 17]. For example, two publications by Lee at al. [15, 17] described the application of fat saturated T2-weighted SEMAC sequences for metal artifact

**Table 2** Average scores with standard deviations for visualization of anatomical structures

| Evaluated structures | Visualization score 1.5 T | Visualization score 3.0 T | Visualization score difference (1.5 T-3.0 T) | $p$ values |
|---|---|---|---|---|
| Greater trochanter | 4.61 | 4.72 | −0.11 | 0.43 |
| Lesser trochanter | 4.56 | 4.44 | 0.12 | 0.35 |
| Femoral N&S | 3.94 | 3.83 | 0.11 | 0.59 |
| Acetabulum | 3.55 | 3.33 | 0.22 | 0.13 |
| Sciatic nerve | 4.39 | 3.89 | 0.5 | 0.13 |
| Obturator muscles | 4.50 | 4.50 | 0 | 1 |
| Iliopsoas muscle | 4.50 | 4.39 | 0.11 | 0.35 |

**Table 3** Average scores with standard deviations for technical evaluation of MAVRIC sequences at 1.5 and 3.0 T; mean differences and *p* values are also provided

| Variables | MAVRIC 1.5 T | MAVRIC 3.0 T | Difference | *p* value |
|---|---|---|---|---|
| Image quality | 4.44 | 4.22 | 0.22 | 0.13 |
| Fat suppression | 3.72 | 2.89 | 0.83 | 0.01 |
| Geometrical distortion | 4.39 | 4.22 | 0.17 | 0.46 |
| Artifacts | 42.15 | 58.8 | −16.6 | <0.001 |

reduction at 3 T. Another recent article from Kretzschmar et. al. [13] described the use of MAVRIC SL on a 3.0 T scanner showing significant reduction of metallic artifacts compared to standard sequences. In addition, improvements were noted in the visualization of bone-prosthesis interface and in the periprothesic area in subjects who underwent spinal fixation surgery. Using MAVRIC SL, our study demonstrated similar visualization of anatomical structures near metal implants at 3.0 T as compared to 1.5 T (Table 2). In general, we found the acetabular area to be the most challenging region at both magnetic field strengths. This is most probably due to the larger volume of high-susceptibility metal (cobalt-chromium alloy) in this area that resulted in very limited and partial visualization of this structure (Table 3). Regarding the detection of pathological abnormalities, MAVRIC-SL at 3.0 T performed equally to MAVRIC-SL at 1.5 T as all abnormalities were noted at both magnetic field strengths (Table 4).

Our study demonstrated that artifacts at 3.0 T had a larger size than at 1.5 T; however, the difference in size of the artifact did not significantly impact the visualization of anatomical or pathological features in our small cohort. There might be some instances where the residual metal artifact size would prevent an accurate diagnosis and, hence, we believe that a larger population would need to be studied to conclusively investigate potential limitations at the higher field strength. However, a recent publication [15] performed in an animal model found similar diagnostic performance in lesion detection using MAVRIC sequences at both field strengths, which is in agreement with the findings of our study.

**Table 4** Pathological abnormalities recorded

| Abnormality detected | No. of abnormalities detected at 1.5 T | No. of abnormalities detected at 3.0 T |
|---|---|---|
| Joint effusion | 9 | 9 |
| Bursitis | 11 | 11 |
| Bone marrow edema pattern | 2 | 2 |
| ALVAL | 2 | 2 |
| Insertion tendinopathy (greater trochanter) | 6 | 6 |
| Osteolysis | 3 | 3 |

**Table 5** Inter- and intra-rater reliability

| | Mean | 95 % CI |
|---|---|---|
| Cohen's K (inter) | 0.79 | (0.62–0.93) |
| Cohen's K (intra) | 0.97 | (0.82–1.0) |
| ICC (inter) | 0.93 | (0.87–0.98) |
| ICC (intra) | 0.99 | (0.98–0.99) |

A substantial difference between the field strengths was related to the fat saturation ability. In our study 3.0 T MAVRIC-SL scored significantly lower than 1.5 T MAVRIC-SL in respect to fat saturation efficiency (Fig. 3), which is due to a number of challenges related to the application of high-bandwidth inversion-recovery-based fat-suppression at 3.0 T. First, inversion-based fat saturation demonstrates shading when the inversion pulse application is compromised by inhomogeneous B1 transmission [18, 19]. This is a well-known problem at 3 T due to the reduced wavelength of applied RF fields. In addition, the presence of metal implants can further increase the level of B1 transmission inhomogeneity [19, 20]. To mitigate this effect, inversion pulses are typically applied using adiabatic excitation principles [19]; however, the broadband adiabatic inversion pulses required for metal artifact reduction such as those used in MAVRIC SL, often are limited by specific absorption rate and RF hardware limits at 3.0. As a result, the sensitivity of these pulses to B1 transmission inhomogeneity is increased relative to their application at 1.5 T. The combination of these various challenges of inversion-based fat suppression around metal implants at 3.0 T explain the increased shading and reduced fat saturation performance relative to the 1.5 T implementation.

Finally, our study demonstrated that there is no significant difference in the scores with regards to geometric distortion and image quality. In order to retain a high-resolution image while at the same time generating smaller geometric distortion artifacts in 3.0 T MRI, we optimized our pulse sequences by increasing the readout bandwidth and reducing the echo time [12, 21, 22].

Image quality was slightly higher at 1.5 T; however, this trend was not significant, likely due to the small sample size and is mostly attributed to the effects discussed in the previous paragraph and the increased off-resonance frequencies at the higher field strength. The lower score for image quality of MAVRIC at 3.0 T was mostly due to blurring which was more evident when compared to the sequence obtained at 1.5 T; however, the abnormalities and the anatomical structures were still similarly appreciated (Fig. 5). The increased blurring at 3.0 T can be partially explained by the reduced T2 of musculoskeletal tissues (ranging from 10–35 % reduction) at 3 T relative to 1.5 T. Proton-density-weighted MAVRIC SL images use an echo train length (ETL) between 16–20. Echo trains of such length are susceptible to some blurring from T2 decay, which explains the increased observed blurring at 3.0 T.

Our study has a number of limitations. The main limitation was the small sample size of only 18 subjects, mostly due to the poor patient compliance with the second scan. However, all subjects were prospectively enrolled, highly selected and had both 1.5 and 3.0 T scans within 21 days. A larger population would have allowed for a larger number of abnormalities and possibly some of these would not have been identified at both field strengths. Furthermore, a larger sample size might have demonstrated increased significance for some parameters. A second minor limitation was the lack of an intraoperative correlation to confirm the pathological findings, but this would have required revision surgery, which was not performed in any of our patients at the time of the data collection. Finally, another potential issue was the heterogeneity of hip prostheses in terms of size and materials, also the small number of subjects in each of these subcohorts did not allow for meaningful comparisons.

In conclusion, this prospective study demonstrated that in a small cohort of subjects with symptomatic hip replacement, MAVRIC-SL sequences were able to effectively reduce metal artifacts at both 1.5 and 3.0 T field strengths without significant differences. In particular, the visualization of anatomical structures and demonstration of pathological abnormalities between the two fields strength was similar. However, previously described advantages of higher magnetic field strengths such as higher image quality were compromised by larger artifact size and more limited fat suppression for the described application of metal artifact reduction.

**Grant support** We thank General Electric Healthcare for research funding and support. This research was in part funded with support from the National Institutes of Health (NIH). Grant numbers include U01 AR059507, R01 AR057336 and P50 AR060752.

**Conflict of interest** All authors except for Dr. Michele Guindani have conflict of interests.

## References

1. Shan L, Shan B, Graham D, Saxena A. Total hip replacement: a systematic review and meta-analysis on mid-term quality of life. Osteoarthr Cartil. 2014;22(3):389–406.
2. Singh JA. Epidemiology of knee and hip arthroplasty: a systematic review. Open Orthop J. 2011;5:80–5.
3. Kurtz S, Ong K, Lau E, Mowat F, Halpern M. Projections of primary and revision hip and knee arthroplasty in the United States from 2005 to 2030. J Bone Joint Surg Am Vol. 2007;89(4):780–5.
4. Iorio R, Healy WL, Warren PD, Appleby D. Lateral trochanteric pain following primary total hip arthroplasty. J Arthroplast. 2006;21(2):233–6.
5. Vicar AJ, Coleman CR. A comparison of the anterolateral, transtrochanteric, and posterior surgical approaches in primary total hip arthroplasty. Clin Orthop Relat Res. 1984;188:152–9.
6. Saito S, Ryu J, Oikawa H, Honda T. Clinical results of Harris-Galante total hip arthroplasty without cement: follow-up study of over five years. Bulletin. 1997;56(4):191–6.
7. Blankenbaker DG, Ullrick SR, Davis KW, De Smet AA, Haaland B, Fine JP. Correlation of MRI findings with clinical findings of trochanteric pain syndrome. Skelet Radiol. 2008;37(10):903–9.
8. Thomas MS, Wimhurst JA, Nolan JF, Toms AP. Imaging metal-on-metal hip replacements: the Norwich experience. HSS J. 2013;9(3):247–56.
9. Olsen RV, Munk PL, Lee MJ, Janzen DL, MacKay AL, Xiang QS, et al. Metal artifact reduction sequence: early clinical applications. Radiographics. 2000;20(3):699–712.
10. Lu W, Pauly KB, Gold GE, Pauly JM, Hargreaves BA. SEMAC: slice encoding for metal artifact correction in MRI. Magn Reson Med. 2009;62(1):66–76.
11. Koch KM, Lorbiecki JE, Hinks RS, King KF. A multispectral three-dimensional acquisition technique for imaging near metal implants. Magn Reson Med. 2009;61(2):381–90.
12. Koch KM, Brau AC, Chen W, Gold GE, Hargreaves BA, Koff M, et al. Imaging near metal with a MAVRIC-SEMAC hybrid. Magn Reson Med. 2011;65(1):71–82.
13. Kretzschmar M, Nardo L, Han MM, Heilmeier U, Sam C, Joseph GB, et al. Metal artefact suppression at 3 T MRI: comparison of MAVRIC-SL with conventional fast spin echo sequences in patients with hip joint arthroplasty. European Radiol. 2015.
14. Choi SJ, Koch KM, Hargreaves BA, Stevens KJ, Gold GE. Metal artifact reduction with MAVRIC SL at 3-T MRI in patients with hip arthroplasty. AJR Am J Roentgenol. 2015;204(1):140–7.
15. Liebl H, Heilmeier U, Lee S, Nardo L, Patsch J, Schuppert C, et al. In vitro assessment of knee MRI in the presence of metal implants comparing MAVRIC-SL and conventional fast spin echo sequences at 1.5 and 3 T field strength. J Magn Reson Imaging. 2014.
16. Yanny S, Cahir JG, Barker T, Wimhurst J, Nolan JF, Goodwin RW, et al. MRI of aseptic lymphocytic vasculitis-associated lesions in metal-on-metal hip replacements. AJR Am J Roentgenol. 2012;198(6):1394–402.
17. Lee YH, Lim D, Kim E, Kim S, Song HT, Suh JS. Usefulness of slice encoding for metal artifact correction (SEMAC) for reducing metallic artifacts in 3-T MRI. Magn Reson Imaging. 2013;31(5):703–6.
18. Garwood M, Ugurbil K, Rath AR, Bendall MR, Ross BD, Mitchell SL, et al. Magnetic resonance imaging with adiabatic pulses using a single surface coil for RF transmission and signal detection. Magn Reson Med. 1989;9(1):25–34.
19. Del Grande F, Santini F, Herzka DA, Aro MR, Dean CW, Gold GE, et al. Fat-suppression techniques for 3-T MR imaging of the musculoskeletal system. Radiographics. 2014;34(1):217–33.
20. Graf H, Steidle G, Martirosian P, Lauer UA, Schick F. Effects on MRI due to altered rf polarization near conductive implants or instruments. Med Phys. 2006;33(1):124–7.
21. Olsrud J, Latt J, Brockstedt S, Romner B, Bjorkman-Burtscher IM. Magnetic resonance imaging artifacts caused by aneurysm clips and shunt valves: dependence on field strength (1.5 and 3 T) and imaging parameters. J Magn Reson Imaging. 2005;22(3):433–7.
22. Farrelly C, Davarpanah A, Brennan SA, Sampson M, Eustace SJ. Imaging of soft tissues adjacent to orthopedic hardware: comparison of 3-T and 1.5-T MRI. AJR Am J Roentgenol. 2010;194(1):W60–4.